Evaluation of the stress-strain uniformities in the direct simple shear device using 3D discrete element modeling

Antone Dabeet, Dharma Wijewickreme & Peter Byrne
Department of Civil Engineering - University of British Columbia, Vancouver, BC, Canada

ABSTRACT

The direct simple shear (DSS) test has been widely used to characterize soil behavior particularly under cyclic loading. Assessing the degree of uniformity of stresses and strains within the DSS specimen is important for the use and interpretation of the results emanating from testing. So far, studies on non-uniformities in the DSS test have been conducted using direct boundary measurements of stresses in laboratory specimens supported with a continuum based analytical approach. With the recent advances in computers, it is now possible to more realistically model soil particles as discrete elements. PFC^{3D} 3.1 (Particle Flow Code developed by *Itasca*) was used in this study to investigate the degree of non-uniformities of stresses and strains in a cylindrical specimen subjected to simple shear boundary conditions. The approach allows for the determination of stresses not only at the boundaries, but also within the DSS specimen. It was found that both shear and normal stresses are non-uniform near the specimen boundaries, with stresses becoming more uniform in the central parts of the specimen. This is in general agreement with findings of previous studies from continuum based analyses and boundary measurements. The computed stress ratios, along the central plane parallel to the direction of shearing, were found to be more uniform compared to the non-uniformity arising from individual stresses; this implies that the stress ratio calculated from average stress measurements is still fairly reliable. The presence of some friction on the lateral walls seems to have little effect on the measured stresses and strains in the specimen during shearing when compared to the ideal case with frictionless lateral boundaries.

RÉSUMÉ

L'essai de cisaillement simple direct (CSD) a été couramment employé pour caractériser le comportement de sol en particulier sous charge cyclique. L'évaluation du degré d'uniformité des contraintes et déformations dans le spécimen dans le CSD est importante pour l'interprétation et usage des résultats émanant de l'essai. Jusqu'ici, les études sur les non uniformitées dans l'essai SCD ont été entreprises utilisant des mesures directes de frontière des efforts dans les spécimens de laboratoire soutenus par une approche analytique basée en continuum. Avec les avances récentes des ordinateurs, il est maintenant possible de modeler plus réalistiquement les particules de sol comme élements discrets. PFC3D 3.1 (code d'écoulement de particules développé par Itasca) a été employé dans cette étude pour étudier le degré de non uniformitées des contraintes et déformations dans un spécimen cylindrique dans des conditions de frontière de cisaillement simple. L'approche permet de déterminer les efforts non seulement aux frontières, mais également dans le spécimen de CSD. On a constaté que le cisaillement et efforts normaux sont non uniformes proches des frontières du spécimen, avec les efforts devenant considérablement uniformes dans les parties centrales du spécimen. C'est résultats sont en général en accord avec des résultats des études précédentes d' analyses basées en continuum et des mesures de frontière. Les rapports de contraintes calculés le long du plan central parallèle à la direction du cisaillement, sont plus uniforme comparés à l'irrégularité résultant des efforts individuels; ceci implique que le rapport de contraintes calculé à partir des mesures moyennes d'effort est encoré assez fiable. La présence de friction sur les murs latéraux semble exercer peu d'effet sur les contraintes et déformations mesurées dans le spécimen comparés au cas idéal de frontières latérales sans friction.

1. INTRODUCTION

The cyclic direct simple shear test (DSS) has been commonly used to assess the earthquake response of soils (Bjerrum and Landva 1966; Wood and Budhu 1980; Finn et al. 1982; Wijewickreme et al. 2005). The test was originally developed in an attempt to overcome major stress non-uniformities imposed by the direct shear (commonly referred to as "shear box") test. Interest in the DSS test has been growing due to its simplicity and its ability to more realistically simulate field stress conditions that involve rotation of principal stresses.

The commonly used types of direct simple shear tests include the cubical specimen type with rigid side boundaries initially developed by Roscoe (1953), and the cylindrical specimen type with the wire-reinforced membrane providing lateral confinement (Bjerrum and Landva 1966). The DSS test with cylindrical specimen has been more commonly in use and is the subject of analysis in this paper.

DSS testing process deviate from the ideal simple shear boundary conditions due to the absence of complementary shear on the lateral boundary; this has been suggested to cause stress non-uniformities within the DSS specimen that can lead to progressive failure. Lucks et al. (1972), from the results of a finite element

(FE) analysis assuming linear elastic soil behavior, concluded that these non-uniformities are local and that 70% of the specimen is under uniform stress conditions under typical loading conditions. Wood and Budhu (1980) presented lab results from DSS testing of Leighton Buzzard sand. Their results showed that stress ratios assessed at the ends of the specimen were similar "on average" to those measured at the center of the specimen, which implied that the effect of stress non-uniformities might not be significant. Saada and Townsend (1981), using the results of a photoelastic study, concluded that the DSS test "cannot claim to yield either reliable stress-strain relations or absolute failure values. At best they can be exploited in comparing descriptively similar soils". Vucetic and Lacasse (1982) reported results on medium-stiff clay obtained from DSS testing conducted for different height to diameter specimens and membrane types. They concluded that "neither the height nor the membrane reinforcement type have any significant influence on the static stress-strain behavior". Budhu (1984) noted that the distribution of strains along the height of the specimen is fairly uniform for shear strains less than 5%.

To the authors' knowledge, previous analytical studies on the stress uniformities in the DSS device have been mainly limited to analysis of continua with the assumption of linear elastic material behavior, which has the potential to overestimate the degree of non-uniformities. Laboratory studies are limited to boundary measurements of stresses. With the recent advances in computers, it is now possible to model soil particles more realistically as discrete elements. This paper presents the results of a discrete element study of stress and strain non-uniformities in a DSS specimen subjected to drained monotonic loading conditions using PFC^{3D} 3.1 (particle flow code in three dimensions developed by *Itasca*). Boundary and internal measurements are presented for stresses and strains.

2 OVERVIEW ON PFC^{3D}

Particle Flow Code in three dimensions (PFC^{3D}) is based on the discrete elements method by Cundall and Strack (1979) and Itasca (2005a). Soil particles are modeled as rigid spheres (referred to as balls). The contacts between balls are modelled using the soft contacts approach that allows particle to virtually overlap (Itasca, 2005b). The magnitude of the overlap is related to the forces at the contacts by the normal and shear stiffness values, K_n and K_s, respectively. These stiffness values have the units of force/displacement. Maximum friction at the contacts can be specified. Slippage occurs if the ratio of shear to normal forces exceeds maximum friction. Boundaries are referred to as walls. The contacts between the balls and walls are modeled in a similar way to contacts between balls. The code uses an explicit solution scheme.

The discrete element method and PFC in particular have been increasingly used in modeling soils (Cheng et al. 2003; Powrie et al. 2005; Pinheiro et al. 2008).

3 ANALYSIS METHODOLOGY

A DSS specimen with a height of 3 cm and a diameter of 10 cm filled with "balls" was considered for the PFC simulation herein, leading to a height to diameter ratio of 0.3. In the simulation, balls were initially formed in a very loose state (not touching) in a cylindrical mould that had the same diameter as the specimen cavity. The locations of the balls were generated randomly inside the mould with particle sizes range that follows a Gaussian distribution (simulated mean diameter of 2.8 mm and with a standard deviation of 0.07). The generated "PFC soil" has a coefficient of uniformity of 1.6.

The soil placement simulation is graphically illustrated in Figure 1. The mould is mounted on top of the sample cavity as shown in Figure 1a. Gravity is then activated and the process of balls falling under gravity and filling the specimen cavity is simulated. This is similar to the air pluviation preparation technique commonly used in soil laboratory testing. At the end of the soil placement phase, particles with centers located above the top of the specimen are deleted and the top cap/boundary is placed. The number of remaining balls that form the specimen is around 12000. The specimen is now ready for consolidation.

The specimen was consolidated by moving the top and bottom boundaries simultaneously at a rate of 2mm/second. The time step was set to around 10^{-6} seconds /computation cycle (i.e. it takes one million computation cycles to displace each of the walls by 2mm). This takes hours to days of processing time depending on the number of balls in the model and the computation power available. Figure 1b shows a side view of the specimen at the end of consolidation.
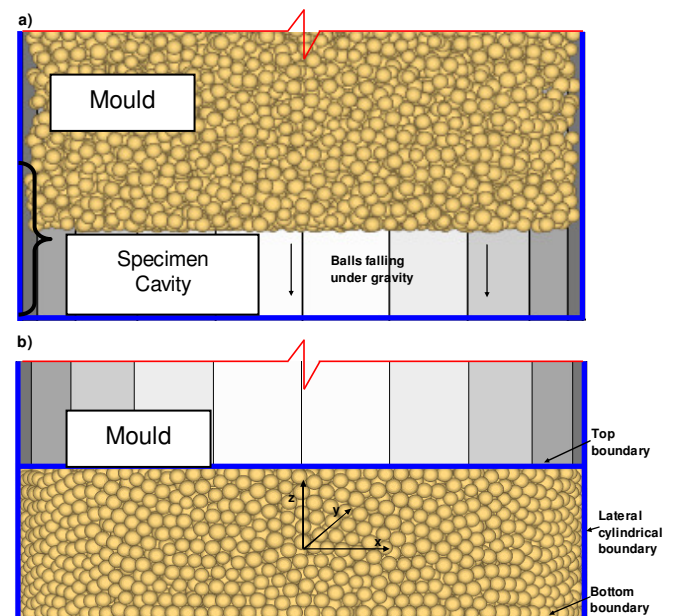

Figure 1. Side view of the PFC specimen a) during sample preparation b) at the end of consolidation.

Average stresses are calculated at the boundaries and at seven locations inside the specimen. Normal stresses on the top and lateral boundaries are equal to the sum of the normal forces acting at the wall-ball contacts divided by the total surface area of the wall. The Measurement Sphere (MS) routine in PFC[3D] is used to calculate local stresses and porosities. The center and radius of each measurement sphere is specified. The MS routine computes the stress tensor from forces at contacts averaged over the volume of the MS. Figure 2 shows cross-sections through the central plane parallel to the direction of shear illustrating the locations and sizes of the measurement spheres. MS 11 through MS 13 (Figure 2b) have centers closer to the top boundary compared to MS 1 through MS 4 (Figure 2a).
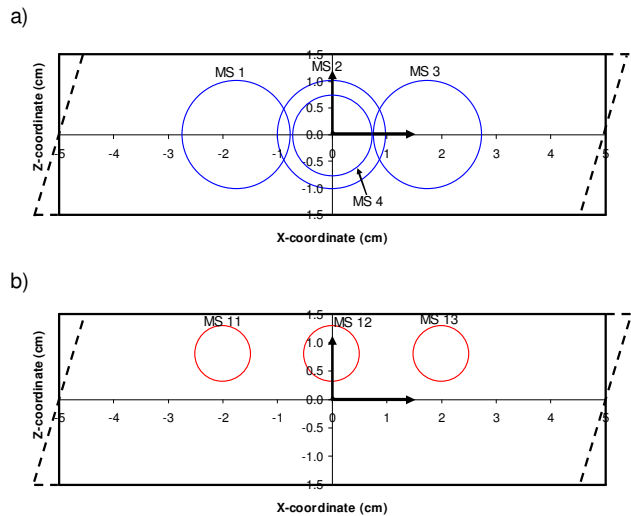
a)

b)

Figure 2. Cross-section through the central plane parallel to shearing direction a) Measurement Spheres 1-4 b) Measurement Spheres 11-13.

The specimen is sheared by rotating the cylindrical lateral boundary around the Y-axis as shown for a cross-section in Figure 2. The top and bottom boundaries are simultaneously displaced horizontally as a function of shear strain in the positive and negative x-directions, respectively. They are allowed to move in the z-direction during drained shearing to maintain the desired σ'_{zz}.

The locations of the centers of balls passing through five vertical sections (i.e. parallel to the Z-axis) at x=0, ±1.75, and ±3.5cm were recorded during shearing. The recorded data was used to assess the variation of shear strain along the x and z coordinates. Shear strains were also monitored at the lateral boundaries.

The boundary shear strain rate used was 2.5rad/sec with a fixed time step of 10^{-6} seconds /computation cycle. An increment of boundary shear strain of 0.00025 is applied by running the code for 100 cycles. For drained shearing, the vertical stress subroutine is then called to correct σ'_{zz} to its pre-shearing value ± a tolerance of 0.5 kPa before another boundary shear strain increment is applied. This is performed by moving the upper and lower boundaries simultaneously.

4 INPUT PARAMETERS FOR NUMERICAL SIMULATION

The normal and shear stiffness parameters at all contacts (ball-ball or ball-wall) were assigned a value of 500 kN/m. Selected stiffness parameters resulted in a reasonable computation time for the analyzed model.

The specimen was consolidated with a ball-ball friction of 0.5 and a zero ball-wall friction to minimize local shear stresses generated during consolidation. This is believed to result in a more uniform specimen at the end of consolidation. During shearing, two ball-ball friction coefficients of 0.5 and 1 were selected for two analysis cases (simulations 1 & 3 in Table 1). The top and bottom wall-ball friction coefficient is given a high value of 10 for all simulations. The lateral wall-ball friction coefficient is assigned a value of 0.5 for case 2. Frictionless contacts at the lateral wall were assumed for all other simulations. The effect of vertical effective stress was investigated for the two values of 100 kPa and 150 kPa. All simulations assume drained conditions.

The specific gravity of the balls is assumed as 2.67. Viscous damping was used with a damping ratio of 0.7.

Table 1. Input parameters and stress conditions for simulations 1-4.

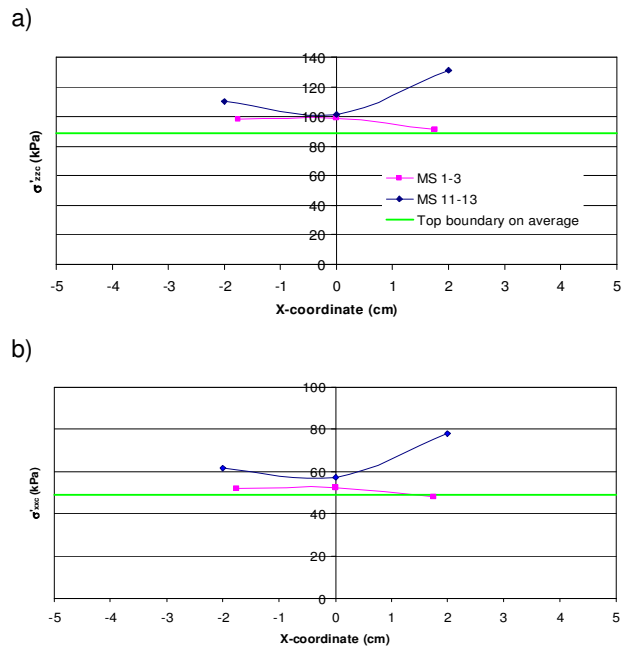| Simulation No.	σ'_{zzc} (kPa)	B-B friction*	Lateral W-B friction*
1	100	0.5	0
2			0.5
3		1	0
4	150	0.5	0

a)

b)

Figure 3: Average stresses on the boundaries and at the measurement spheres after consolidation and before shearing a) vertical effective stress σ'_{zzc} b) horizontal/lateral effective stress σ'_{xxc}.

5 SIMULATIONS RESULTS

5.1 Stresses at the End of Consolidation

End of consolidation normal and lateral stresses at the boundaries and at the measurement spheres on average are shown in Figure 3. Each point in the plot represents the center of a measurement sphere. It is reasonable to expect that the core of the specimen (MS 1 through MS 3) would be the least affected by non-uniformities caused by the boundaries. It was decided to assess the stress conditions at the selected locations when the value of vertical stress (σ'_{zz}) at the central measurement sphere (MS 2) reached a value of 100 kPa, and the results in Figure 3a express the computed σ'_{zz} values for that selected case. As may be noted, the observed variation in stresses can be attributed to the local non-uniformities arising from boundary effects. As expected, the distribution of σ'_{zz} for MS 1 through MS 3, which represent locations along the core of the specimen, on average is relatively more uniform (i.e., less variation with x-coordinate) and also closer to the average stresses estimated at the specimen boundary based on boundary measurement. .

The stress values presented in Figure 3b show similar trends with regards to lateral stress (σ'_{xx}) non-uniformities. The average σ'_{xx} value at the boundary is very close to the computed σ'_{xx} values at MS1 through MS 3. A typical value for the lateral stress coefficient of around 0.5 was calculated from MS1 through MS 3 and from boundary stresses. Void ratios averaged at each of the locations MS 1, MS 2, and MS 3 are 0.563, 0.573, and 0.586, respectively.

5.2 Shear Strain Non-uniformities

The interpretation of particle movements in the x-direction during shearing provides an opportunity to assess strains along the specimen height. The x-displacements of 13 randomly selected balls initially (pre-shearing state) aligned along the z-axis near x=0, during simulation 1 are presented in Figure 4. Each point on the figure represents the location of the center of a particle when the boundary strain is at 10%. The distribution of the particles locations shows only a slight variation from the ideal linear trend. Hence, for simplicity, it was assumed that a linear approximation yields a representative value for an average strain. Similar uniform strain trends along the z-axis were observed for other X values. The interpretation of the following results is based on average strain values along the height of the specimen. A reasonably uniform shear strain conditions along the z-axis (i.e., along the specimen height) can be interpreted from this assessment. The interpretation of the following results is based on average strain values computed as per above along the height of the specimen.
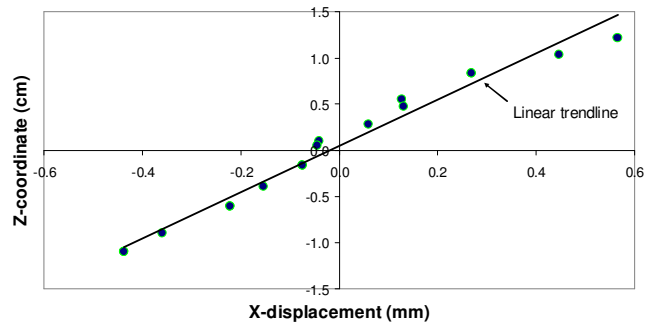

Figure 4. X-displacements of a group of balls initially (pre-shearing) aligned along the Z-axis near x=0 (simulation 1).
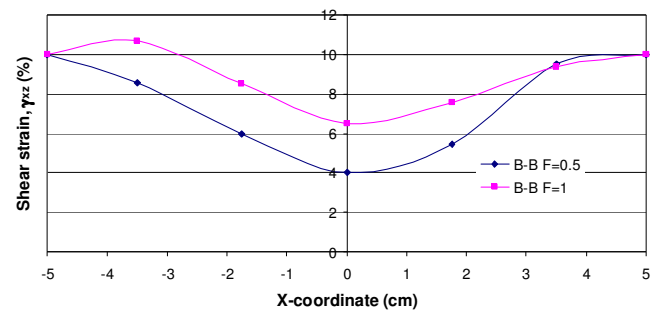

Figure 5. Distribution of shear strains along the X-coordinate.

Figure 5 was produced by calculating strains from particle displacements at different x-locations near y=0 when the boundary strain was at 10% for the simulations 1 & 3. Minimum shear strain seems to occur at the center of the specimen in both simulations. It is important to note that the strains are more uniform along the Z-coordinate for simulation 3 which was conducted with a higher B-B friction (F=1) compared to simulation 1, which was conducted with F =0.5.

5.3 Stress Non-uniformities During Shearing

Average shear stress development with increasing strain, at locations MS 1 through MS 4, are shown Figure 6a. It is noted that the shear strains represented in the x-axis are the average strains as discussed in the previous section. The plots for the cases MS 2 & 4, which are computed from two zones that are at the very center of the specimen are very similar; this confirms the uniformity of stresses within the central zone.

The stresses plotted in Figure 6b shows that the computed vertical stresses for MS 2 & 4 are similar further confirming the uniform stress conditions at the core. Normal stress increases with shearing to a maximum of 136kPa for MS 1. For MS 3, normal stress initially decreases with shearing. It then slightly increases at shear strain of 1.5% to a steady value of about 83kPa.
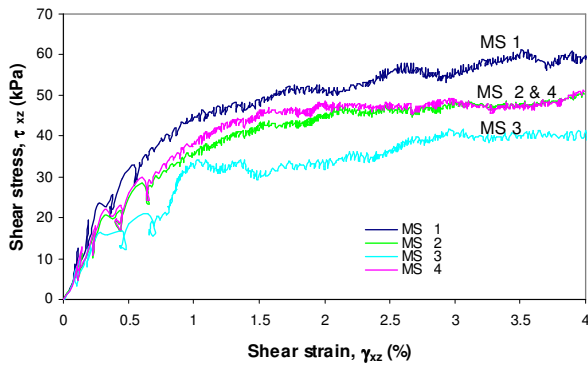
The stress ratio versus shear strain behavior shown in Figure 7 was plotted after normalizing the shear stress values in Figure 6 by the corresponding normal stresses.

The results in the plot indicate relatively uniform stress ratio development with strain across the specimen for MS 1 through MS 4.

5.4 Effect of Vertical Effective Stress

Stress ratio versus shear strain relations obtained from simulations 1 & 4 with σ'_{zz} of 100 kPa and 150 kPa, respectively, are shown in Figure 8a. Although slightly stiffer response can be noted in simulation 1, the stress ratio versus shear strain relations for the simulations conducted at the two σ'_{zz} values of 100 kPa and 150kPa are remarkably similar.
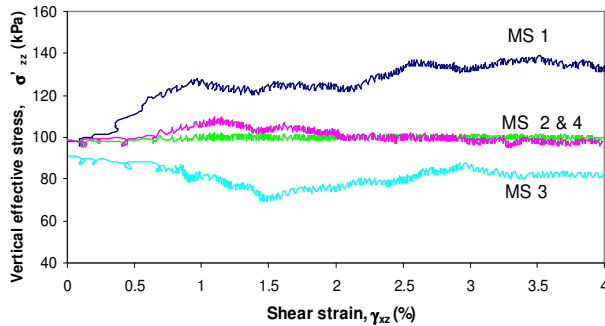
a)

b)

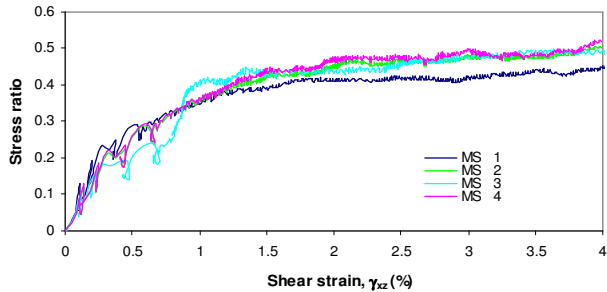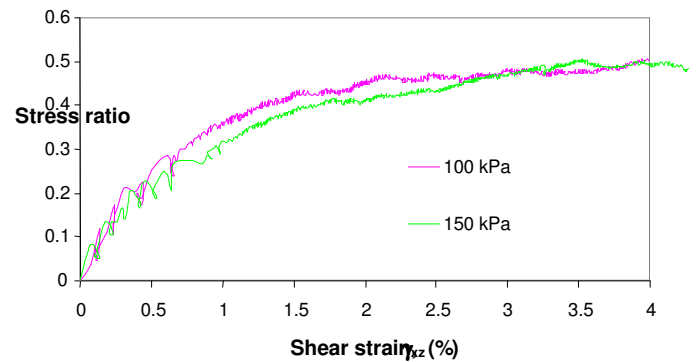Figure 6. Stress vs. shear strain response for simulation number 1 a) shear stress, τ_{xz} b) vertical effective stress, σ'_{zz}.

Figure 7. Stress ratio (τ_{xz}/σ'_{zz}) vs. shear strain for simulation number 1.

The volumetric strain versus shear strain relations obtained from simulations 1 & 4 with σ'_{zz} of 100 kPa and 150 kPa, respectively, are presented in Figure 8b. A typical more contractive behavior was observed for simulation 4 with the higher vertical effective stress (see Figure 8b), which is in accord with the expected increase in shear contractiveness with increasing confinement.

5.5 Effect of Side Boundary Friction

The stress ratio versus shear strain response obtained from simulations 1 & 2 are plotted in Figure 9. A softer response and a smaller maximum stress ratio were observed for simulation 1 with frictionless side boundary. The difference in stress ratio between the two simulations at shear strain of 4% is 0.06.
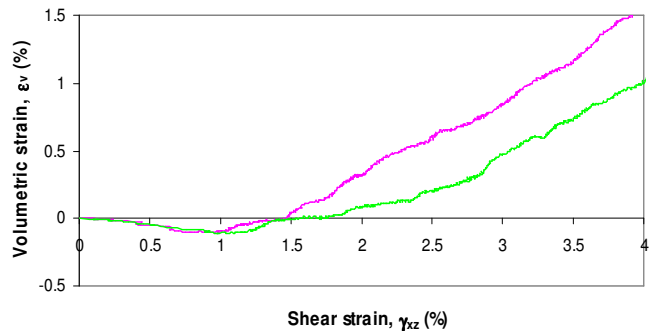
a)

b)

Figure 8. Simulations 1 and 4 (results for MS 2) a) shear stress strain b) volumetric strain vs. shear strain.
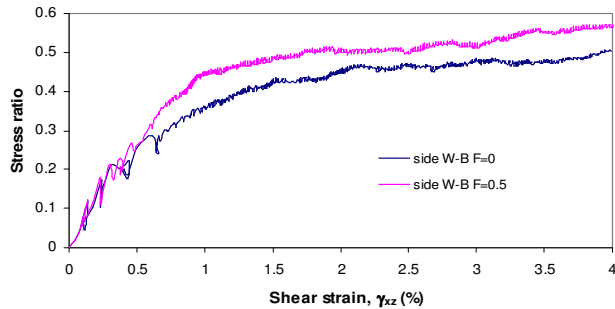
197

Figure 9: Effect of lateral wall friction on the stress ratio vs. shear strain response (simulations 1 & 2).

6 DISCUSSION OF ANALYSIS OUTCOME

As noted from the foregoing, the stresses determined by considering spherical zones closer to the specimen boundary yielded a relatively non-uniform state of stress at the end of consolidation compared to the middle/central measurement spheres. It seems that the use of boundary measurement of stresses can result in overestimating non-uniformities. Airey and Wood (1984) and Budhu (1984b) presented lab results showing the distribution of vertical stresses at the end of consolidation for different sands and side boundary stiffnesses. Their results showed highly non-uniform end of consolidation stress distributions from boundary local measurements.

Budhu (1984a), based on data from monitoring the change in positions of lead shots during shear, noted the presence of non-uniform strain distributions along the height of the specimen. The non-uniformities, in particular, were large for strains higher than 5%. In contrast, significant strain non-uniformities along the height (Z-coordinate) were not observed from the current PFC modeling for the range of strains investigated. Note that rigid side boundaries were used in the PFC model which is different from the wire-reinforced membrane used in the lab test. The inadequate stiffness of the membrane can impose non-uniform boundary strain conditions (Youd 1972).

The strain distributions shown in Figure 5 suggest that the non-uniformities are reduced for the higher B-B friction of 1 compared to the case of B-B friction of 0.5. This implies that the non-uniformities could accentuate when there is more opportunity for particle slippage.

The specimen that initially (pre-shearing) had relatively uniform vertical stress conditions (e.g., for simulations MS 1 through 3) experienced non-uniformities during the shearing process. However, the stresses at the core were assessed to be still uniform (e.g. shear stress strain plots for MS2&4 are very similar).

The stress ratios observed along the central plane parallel to the direction of shearing (i.e., MS 1 through MS 4) are more uniform than individual stresses which implies that stress ratio calculated from average stress measurements should be still fairly reliable. Wood and Budhu (1980) showed, for Leighton Buzzard Sand, similar stress ratio shear strain response from an average measurement and from a measurement at the center, with the former showing a slightly weaker response.

7 CONCLUSIONS

A 3D discrete element analysis of the DSS testing process was performed using PFC[3D] software to investigate non-uniformities of stresses and strains in cylindrical DSS specimens. The initial particle arrangement for the simulation was achieved by numerically "raining" spherical particles under gravity, followed by consolidation and shearing phases.

The findings of this study are:
- It appears that local boundary measurements of stresses can result in overestimating stress non-uniformities compared to those assessed from computed internal stresses at zones closer to the center of the specimen. Internal stresses were close to the average stresses computed at the top boundary of the specimen.
- Shear strains were found to be reasonably uniform along the height of the central part of the specimen for the range of strains investigated.
- Strain non-uniformities were noted to accentuate when there is opportunity for particle slippage. The effect of slippage can be numerically investigated by changing B-B friction.
- Although individual stresses distributions during shearing are non uniform, stress ratio distribution was found to be remarkably uniform for all the simulations conducted.
- The well known expected increase in shear contractiveness with increasing confinement was also reflected in the results of numerical simulation supporting the suitability of the PFC modeling.

From the above results, it can be seen that the DEM and PFC[3D] in particular are powerful tools that can be used in evaluating soil element tests which is important for the use and interpretation of the results. It was shown that PFC[3D] captures the main characteristic of soil constitutive behavior for drained simple shear boundary conditions under monotonic shearing.

REFERENCES

Airey, D.W., and Wood, D.M. 1984. Discussion of specimen size effect in simple shear test, by Vucetic, M., and Lacasse, S. *Journal of the Geotechnical Engineering Division*, 110:439-442.

Bjerrum, L., and Landva, A. 1966. Direct simple shear tests on a Norwegian quick clay. *Geotechnique*, 16:1-20

Budhu, M. 1984a. Nonuniformities imposed by simple shear apparatus. *Canadian Geotechnical Journal*, 20: 125-137.

Budhu, M. 1984b. Discussion of specimen size effect in simple shear test, by Vucetic, M., and Lacasse,S.

Journal of the Geotechnical Engineering Division, 110: 442-445.

Cheng, Y.P., Nakata, Y., and Bolton, M.D. 2003. Discrete element simulation of crushable soil. *Geotechnique*, 53: 633-641.

Cundall, P.A., and Strack, O.D.L. 1979. A discrete numerical model for granular assemblies. *Geotechnique*, 29: 47-65.

Dyvik, R., Zimmie, T. F., and Floess, C. H. L. 1981. Lateral stress measurement in direct simple shear device. In *Laboratory Shear Strength of Soil*, ASTM STP 740:191-206.

Finn, W.D.L., Bhatia, S.K., and Pickering D.J. 1982. The cyclic simple shear test. In *Soil Mechanics- Transient and Cyclic Loads*. John Wiley & Sons Ltd., 583-607.

Itasca Consulting Group, Inc. 2005a. PFC[3D] (Particle Flow Code in Three Dimensions), Version 3.1. Minneapolis, USA.

Itasca Consulting Group, Inc. 2005b. PFC[3D] user manual. Minneapolis, USA.

Lucks, A., Christian, J., Brandow, E., and Hoeg, K. 1972. Stress conditions in NGI simple shear test. *Journal of the Soil Mechanics and Foundations Division*, 98:155-160.

Pinheiro, M., Wan, R., and Li, Q. 2008. Drained-undrained response and other fundamental aspects of granular materials using DEM. *Canadian Geotechnical Conference*, Edmonton: 224-231.

Powrie, W., Ni, Q., Harkness, R., and Zhang, X. 2005. Numerical modeling of plane strain tests on sands using a particulate approach. *Geotechnique*, 55: 297-306.

Roscoe, K.H. 1953. An apparatus for the application of simple shear to soil samples. *Proc. 3rd Int. Conf. Soil Mech.*, Zurich: 186-191.

Saada, A. S., and Townsend, F. C. 1981. State of the art: Laboratory strength testing of soils. In *Laboratory Shear Strength of Soils*. American Society for Testing and Materials: 7-77.

Vucetic, M., and Lacasse, S. 1982. Specimen size effect in simple shear test. *Journal of the Geotechnical Engineering Division*, 108:1567-1585.

Wijewickreme, D., Sriskandakumar, S., and Byrne, P.M. 2005.Cyclic loading response of loose air-pluviated Fraser River Sand for validation of numerical models simulating centrifuge tests. *Canadian Geotechnical Journal*, 42: 550-561.

Wood D.M., and Budhu, M. 1980. The behaviour of Leighton Buzzard Sand in cyclic simple shear tests. *International Symposium on Soils under Cyclic and Transient Loading*, A. A. Balkema, Rotterdam: 9-21

Youd, T.L. 1972. Compaction of sand by repeated shear straining. *Journal of Soil Mechanics and Foundations Division*, 98: 709-725.